



# THE UNIVERSITY *of* EDINBURGH

## Edinburgh Research Explorer

### Locating Gases in Porous Materials: Cryogenic Loading of Fuel Related Gases Into a Sc-based Metal-Organic Framework under Extreme Pressures

**Citation for published version:**

Sotelo, J, Woodall, CH, Allan, DR, Gregoryanz, E, Howie, RT, Kamenev, K, Probert, MR, Wright, PA & Moggach, S 2015, 'Locating Gases in Porous Materials: Cryogenic Loading of Fuel Related Gases Into a Sc-based Metal-Organic Framework under Extreme Pressures' *Angewandte Chemie International Edition*, vol. 54, no. 45, pp. 13332–13336. DOI: 10.1002/anie.201506250

**Digital Object Identifier (DOI):**

[10.1002/anie.201506250](https://doi.org/10.1002/anie.201506250)

**Link:**

[Link to publication record in Edinburgh Research Explorer](#)

**Document Version:**

Peer reviewed version

**Published In:**

*Angewandte Chemie International Edition*

**General rights**

Copyright for the publications made accessible via the Edinburgh Research Explorer is retained by the author(s) and / or other copyright owners and it is a condition of accessing these publications that users recognise and abide by the legal requirements associated with these rights.

**Take down policy**

The University of Edinburgh has made every reasonable effort to ensure that Edinburgh Research Explorer content complies with UK legislation. If you believe that the public display of this file breaches copyright please contact [openaccess@ed.ac.uk](mailto:openaccess@ed.ac.uk) providing details, and we will remove access to the work immediately and investigate your claim.



# Locating Gases in Porous Materials: Cryogenic Loading of Fuel Related Gases Into a Sc-based MOF under Extreme Pressures

Jorge Sotelo,<sup>[a]</sup> Christopher H. Woodall,<sup>[b]</sup> Dave R. Allan,<sup>[e]</sup> Eugene Gregoryanz,<sup>[c]</sup> Ross T. Howie,<sup>[c]</sup> Konstantin V. Kamenev,<sup>[b]</sup> Michael R. Probert,<sup>[d]</sup> Paul A. Wright,<sup>[f]</sup> and Stephen A. Moggach<sup>[a]\*</sup>

**Abstract:** An alternative approach to loading metal organic frameworks with gas molecules at high (kbar) pressures is reported. The technique, which uses liquefied gases as pressure transmitting media within a diamond anvil cell along with a single-crystal of a porous metal organic framework, is demonstrated to have considerable advantages over other gas-loading methods when investigating host-guest interactions. Specifically, loading the metal organic framework  $\text{Sc}_2\text{BDC}_3$  with liquefied  $\text{CO}_2$  at 2 kbar reveals the presence of three adsorption sites, one previously unreported, and resolves previous inconsistencies between structural data and adsorption isotherms. A further study with supercritical  $\text{CH}_4$  at 3 – 25 kbar demonstrates hyperfilling of the  $\text{Sc}_2\text{BDC}_3$  and two high pressure displacive and reversible phase transitions are induced as the filled MOF adapts to reduce the volume of the system.

Understanding how guest molecules in metal-organic framework (MOFs) interact with each other and the framework they occupy upon adsorption is vital for the development and commercial application of MOFs, for example in carbon capture and gas sequestration technologies.<sup>[1]</sup> Spectroscopic techniques, such as IR<sup>[2]</sup> and solid state NMR<sup>[3]</sup> are often used for probing these interactions. Crystallographic studies, both X-ray and neutron, utilizing various environmental cells have proven invaluable in determining the nature of host-guest interactions within MOFs and their guest-driven structural flexibility.<sup>[4]</sup> This is particularly important in the many cases where the uptake behavior, which can include conformational changes in the framework itself, can be perturbed by the type and amount of guest adsorbed.<sup>[5]</sup> One of the main reasons why so little data is available is that the experimental location of gas molecules in

MOFs is challenging. The gas molecules are often disordered and exhibit thermal motion which is difficult to model crystallographically even when cooled close to the freezing temperature of the gas adsorbed. *In-situ* cells have been developed for collecting crystallographic data whilst exposing a MOF to a gaseous environment at tens, or even hundreds of bars of pressure in an effort to saturate the pores with gas molecules, though even here, the gas molecules are often difficult to observe experimentally. For these reasons, despite the intensive research in carbon capture technologies, relatively few crystallographic studies have been reported where  $\text{CO}_2$  molecules have been unambiguously located within MOFs.<sup>[6]</sup>

The use of condensed gases as pressure transmitting media (PTM) in diamond anvil cells is commonplace in the fields of condensed matter physics and high-pressure mineralogy due to their excellent hydrostatic properties at very high-pressures (> 10 GPa) relative to common liquid PTMs.<sup>[7]</sup> He, Ar and Ne are typically used because they are chemically inert, whilst other gases have been studied for their diverse structural behavior. High temperature and pressure phases of  $\text{CO}_2$  and  $\text{CH}_4$  are of interest for understanding planetary interiors, for example,<sup>[8]</sup> while the formation and decomposition of methane-hydrates, which are only stable at pressure, has been studied in great detail.<sup>[9]</sup> Both  $\text{CO}_2$  and  $\text{CH}_4$  are of obvious industrial and environmental interest.

Here, we present a high-pressure study of the MOF  $\text{Sc}_2\text{BDC}_3$  (BDC = benzene-1,4-dicarboxylate) using both  $\text{CO}_2$  and  $\text{CH}_4$  as PTM. Recent work has demonstrated the active role that PTMs play in high-pressure studies of porous materials, where the ability of the PTM to penetrate the framework can be used to “hyperfill”<sup>[10]</sup> the pores. For example, in a previous study of  $\text{Sc}_2\text{BDC}_3$  using methanol as a PTM, the pores were hyperfilled with methanol molecules at 16 kbar, achieving a density 2.5 times larger than possible under ambient pressure conditions.<sup>[11]</sup> Furthermore, a previous high-pressure study on the zeolitic imidazolate framework, ZIF-8 ( $\text{Zn}(\text{Melm})_2$ , Melm = 2-methylimidazole), revealed a previously unobserved framework conformation, which has since been used to explain a step in its adsorption isotherm observed for a number of gases, and the increased loading capacity on increasing gas pressure.<sup>[12]</sup>

In the case of  $\text{Sc}_2\text{BDC}_3$ , gas cell structural work and isotherms by Miller *et al.* using both  $\text{CO}_2$  and  $\text{CH}_4$  revealed interesting features worthy of further investigation.<sup>[13]</sup> Adsorption of  $\text{CO}_2$  into  $\text{Sc}_2\text{BDC}_3$  at 1 bar and 235 K causes a phase transition, which results in a change in space group symmetry from  $Fddd$  to  $C2/c$ . The transition is characterized by a subtle rotation of one of the two symmetry independent BDC linkers upon exposure to  $\text{CO}_2$ . This results in three symmetry independent linkers (Group 1, 2a and 2b) and gives rise to two crystallographically independent channels with one absorption site in each channel (Site 1 and Site 2, Figure 1a). Site 1 lies across two Group 2a linkers with host-

[a] Mr. J. Sotelo, Dr. S. A. Moggach  
EaStChem School of Chemistry and Centre for Science at Extreme Conditions, University of Edinburgh, David Brewster road, Joseph Black Building, Edinburgh EH9 3FJ (UK)  
E-mail: [smoggach@staffmail.ed.ac.uk](mailto:smoggach@staffmail.ed.ac.uk)

[b] Dr. C.H. Woodall  
School of Engineering and Centre for Science at Extreme Conditions, University of Edinburgh, Peter Gurthrie Tait Road, Erskine Williamson Building, EH9 3FD (UK)

[c] Dr. R. T. Howie  
School of Physics and Centre for Science at Extreme Conditions, University of Edinburgh, Peter Gurthrie Tait Road, Erskine Williamson Building, EH9 3FD (UK)

[d] Dr. Michael R. Probert  
School of Chemistry, Newcastle University, Newcastle upon Tyne, NE1 7RU (UK)

[e] Dr. D. R. Allan  
School of Chemistry, Newcastle University, Newcastle upon Tyne, NE1 7RU (UK)

guest C-H...O distances of ca. 2.9 Å and Site 2 is disordered over two positions and also has close C-H...O contacts that range from 2.78 to 2.98 Å. At 235 K and 1 atm. Site 1 and Site 2 are fully and half-occupied, respectively, giving a calculated CO<sub>2</sub> adsorption capacity of ≈ 3 mmol g<sup>-1</sup>, which differs significantly from the experimentally measured maximum uptake of 6.5 mmol g<sup>-1</sup> from adsorption isotherm data.

In our current study, CO<sub>2</sub> was compressed to a pressure of 2 kbar within a modified Merrill-Basset DAC, using a multistate gas compressor containing a single crystal of Sc<sub>2</sub>BDC<sub>3</sub> (SI-I). Single-crystal X-ray analysis revealed that upon sealing the DAC, CO<sub>2</sub> entered the MOF, immediately inducing the expected *Fddd* to *C2/c* phase transition. At 2 kbar, CO<sub>2</sub> positions appeared similar to those previously observed by Miller et al., with both Site 1 and Site 2 occupied (Figure 1A). At 2 kbar, Site 1 was fully occupied,

and Site 2 was observed to have an occupancy refining to 0.83(3).<sup>[13]</sup> The partial occupancy of Site 2 had in previous studies been justified as a form of static disorder, where the two symmetry-related positions of Site 2 could not be occupied simultaneously due to short (<2.2 Å) intermolecular O-O distances. In the high pressure structure we report here, the distance between the two symmetry equivalent sites increased to 2.46 Å, which allows for an increased occupancy for CO<sub>2</sub> at Site 2.

Additionally, a previously undiscovered CO<sub>2</sub> site (Site 3) was observed in the same channel as Site 1 (Figure 1B). Site 3 was modelled in two orientations, disordered over a two-fold rotation axis. Both positions lie very close to each other (<0.2 Å apart), discarding the possibility of both being occupied simultaneously. This was confirmed by the refinement of occupancies in the two

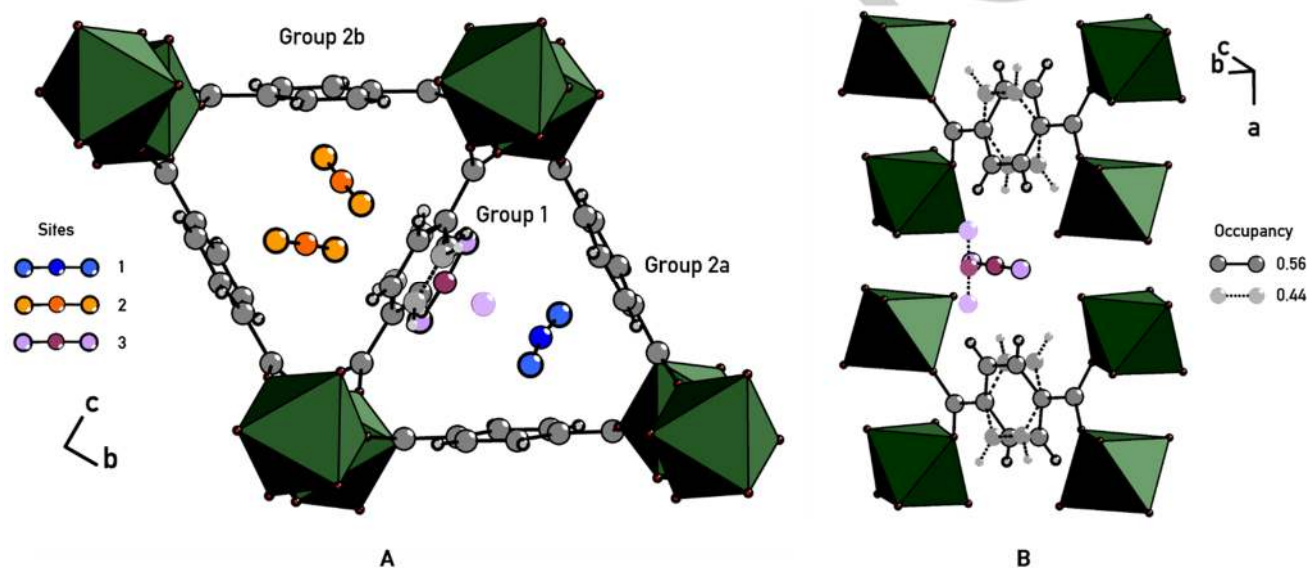


**Figure 1.** Two different views of the CO<sub>2</sub> included structure of Sc<sub>2</sub>BDC<sub>3</sub>. (A) Shows the positions of the three different adsorption sites (Site 1 in blue, Site 2 in yellow and Site 3 in lilac) as well as the disorder in the framework of Group 1. (B) Depicts the positional disorder of Site 3 and the Group 1 BDC linker with solid features representing an occupancy of 0.56 and dashed 0.44.

**Table 1.** Main crystallographic information for the different phases of Sc<sub>2</sub>BDC<sub>3</sub> as synthesised, with CO<sub>2</sub> and CH<sub>4</sub> at different pressures.

	Sc <sub>2</sub> BDC <sub>3</sub>	Sc <sub>2</sub> BDC <sub>3</sub> ·CO <sub>2</sub> - 2 kbar	Sc <sub>2</sub> BDC <sub>3</sub> ·CH <sub>4</sub> - 3 kbar	Sc <sub>2</sub> BDC <sub>3</sub> ·CH <sub>4</sub> - 13 kbar	Sc <sub>2</sub> BDC <sub>3</sub> ·CH <sub>4</sub> - 25 kbar
Unit cell parameters (Å)	<i>a</i> = 8.7458(3) <i>α</i> = 90 <i>b</i> = 20.7439(6) <i>β</i> = 90 <i>c</i> = 34.349(9) <i>γ</i> = 90 <i>V</i> = 6231.7(50) Å <sup>3</sup>	<i>a</i> = 8.693(4) <i>α</i> = 90 <i>b</i> = 34.192(16) <i>β</i> = 111.292(5) <i>c</i> = 11.055(5) <i>γ</i> = 90 <i>V</i> = 3062(2) Å <sup>3</sup>	<i>a</i> = 8.8524(12) <i>α</i> = 90 <i>b</i> = 20.7005(19) <i>β</i> = 90 <i>c</i> = 34.1938(32) <i>γ</i> = 90 <i>V</i> = 6266(1) Å <sup>3</sup>	<i>a</i> = 8.8824(7) <i>α</i> = 90 <i>b</i> = 61.2475(33) <i>β</i> = 90 <i>c</i> = 33.6891(20) <i>γ</i> = 90 <i>V</i> = 18328(2) Å <sup>3</sup>	<i>a</i> = 8.905(2) <i>α</i> = 90 <i>b</i> = 32.501(7) <i>β</i> = 112.05(1) <i>c</i> = 10.675(2) <i>γ</i> = 90 <i>V</i> = 2864(1) Å <sup>3</sup>
Space Group	<i>Fddd</i>	<i>C2/c</i>	<i>Fddd</i>	<i>Fdd2</i>	<i>P2<sub>1</sub>/c</i>
Wavelength (Å)	0.71 (Mo K $\alpha$ )	0.56 (Ag)	0.71 (Mo K $\alpha$ )	0.69 (Zr)	0.69 (Zr)
Completeness	100%	69%	61%	71%	58%
Resolution (Å)	0.84	0.84	0.84	0.84	1.17
R1	0.035	0.107	0.049	0.065	0.145
% SAV <sup>[a]</sup>	35.7	-	37.4	34.8	29.3
Guest uptake	-	6.2 mmol g <sup>-1</sup>	7.8 mmol g <sup>-1</sup>	10.2 mmol g <sup>-1</sup>	-

<sup>[a]</sup>SAV = Solvent Accessible Volume as calculated using Mercury

## COMMUNICATION

orientations – 0.58(4) when the CO<sub>2</sub> molecule is aligned perpendicular to the channels, and 0.42(4) when parallel to it. Both Site 3 positions lie between sets of Group 1 BDC linkers. The close C-H...O contacts between the phenyl rings and the CO<sub>2</sub> induces a disorder of the Group 1 BDC linkers, which also appear in two orientations (Figure 1B, SI-III). Refinement of the occupancy of the two orientations of the linker closely matches the obtained values for Site 3 CO<sub>2</sub> molecules (i.e. 0.56(4) and 0.44(4)) – indicating the disorder is induced by the presence of the new CO<sub>2</sub> site.

By modelling the new Site 3 and the re-ordering of Site 2, the calculated uptake of CO<sub>2</sub> in Sc<sub>2</sub>BDC<sub>3</sub> equates to 6.2 mmol g<sup>-1</sup>. This value is much closer to the maximum capacity of 6.5 mmol g<sup>-1</sup> reported by Miller *et al.*, and much better than their previous estimate from their structural work (of 3.4 mmol g<sup>-1</sup>). This approach also provides direct structural evidence of the expected packing re-arrangement of guest molecules required to reach maximum CO<sub>2</sub> capacity. Application of further pressure beyond 6 kbar resulted in a significant loss of diffraction, most likely due to the freezing of CO<sub>2</sub>. Nevertheless, the structural data already obtained exemplified the use of liquefied, near supercritical gases, as an excellent method for “hyper-filling” MOFs, to the extent of allowing the location of all the adsorption sites, including ones not previously visible with X-ray diffraction.

Before, on uptake of CH<sub>4</sub>, no phase transition was observed, with the framework retaining the orthorhombic *Fddd* symmetry.<sup>[13]</sup> At 9 bar and 230 K, a low affinity for CH<sub>4</sub> was observed, with two crystallographically-distinct adsorption sites, showing very low fractional occupancy for the C-atom (refined values of 0.15 and 0.25 were obtained for Sites 1 and 2 respectively). This implied that there was potential available capacity in the channels for

further adsorption, and motivated us to perform a high-pressure experiment on Sc<sub>2</sub>BDC<sub>3</sub> with CH<sub>4</sub> as the PTM.

CH<sub>4</sub> was loaded using a similar principle to CO<sub>2</sub> but using a different method: cryogenically cooling CH<sub>4</sub> to liquefy into the sample chamber of a standard Merrill-Bassett DAC before sealing at 3 kbar (SI-II). The initial loading showed the immediate inclusion of CH<sub>4</sub> molecules inside the framework, and two adsorption sites were found in similar positions to those previously reported but now fully occupied.<sup>[13]</sup> Site 1 was close to the Group 1 linker (C-H...H-C shortest contact of 2.62 Å), and Site 2 and its symmetry equivalent positions appeared next to Group 2 linkers (C-H...H-C shortest contact of 2.44 Å). Refinement of CH<sub>4</sub> molecules including the hydrogen positions was possible, a rarity in gas adsorption structural studies, and even rarer for high-pressure phases of CH<sub>4</sub> at much higher pressures, where the molecules tend to show several rotational degrees of freedom.<sup>[14]</sup> The data collected at 3 kbar provided an excellent model for the estimation of the adsorbed CH<sub>4</sub> from the refined occupancies (0.91(2) for Site 1 and 0.68(2) for Site 2) corresponded to 7.8 mmol g<sup>-1</sup>, beyond the uptake capacity of 6.8 mmol g<sup>-1</sup> previously reported for Sc<sub>2</sub>BDC<sub>3</sub>. The increased uptake shown here, beyond what was measured previously provides evidence of hyper-filling the framework at elevated pressures.

It was possible to continue the compression study to 25 kbar before freezing of the CH<sub>4</sub> occurred, resulting in a loss of hydrostaticity and deterioration of diffraction quality. Up until 10 kbar the framework remained unaltered, with CH<sub>4</sub> occupancy of both sites increasing until all sites were fully occupied, yielding a maximum capacity of 10.7 mmol g<sup>-1</sup>. A small increase in the unit cell volume of <1% was observed at 3 kbar, which is a frequent observation in other high-pressure inclusion studies on other MOFs including Sc<sub>2</sub>BDC<sub>3</sub>.<sup>[11, 15]</sup> As seen with the inclusion of

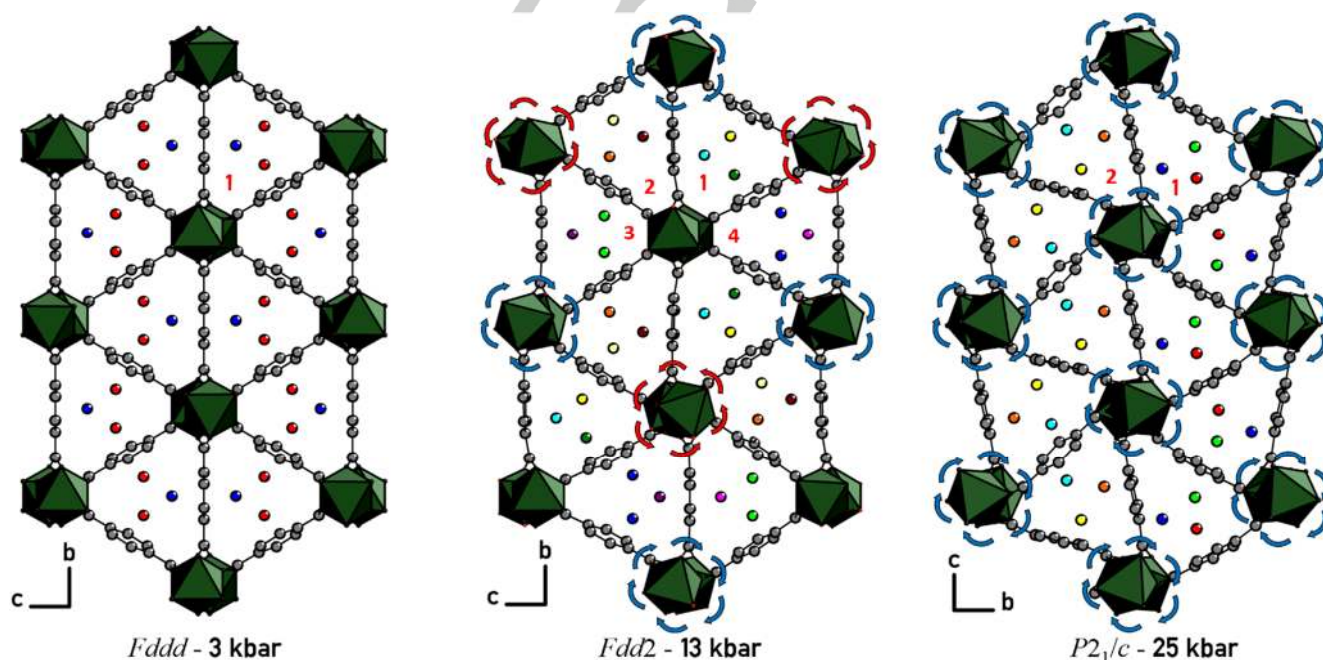


**Figure 2.** Structural transitions upon high-pressure compression of Sc<sub>2</sub>BDC<sub>3</sub> in CH<sub>4</sub>. Red and blue arrows represent the rotation of the ScO<sub>6</sub> octahedra for each phase, with red representing anti-clockwise motion and blue clockwise. CH<sub>4</sub> adsorption sites are coloured by symmetry equivalence, with 2, 10, and 6 independent sites in the *Fddd* (left), *Fdd2* (middle) and *P2<sub>1</sub>/c* (right) respectively. Red numbers represent the different channel types present in each phase change.

methanol, the expansion seemed to rely mostly on an increase along the *a*-axis, which corresponds to the channel directions (SI-IV). The continued increase of the *a*-axis with increasing pressure is in line with further CH<sub>4</sub> being forced inside the framework, but overall the unit cell volume started to decrease above 6 kbar.

At 10 kbar, an increase in the libration of both Group 1 and 2 BDC linkers was observed, suggesting both linkers were adopting more than one orientation. On increasing pressure to 12 kbar, the appearance of weak reflections indicate the onset of a phase change, which is clear at 13 kbar and results in a tripling of the *b*-axis and reduction in symmetry to *Fdd2* (SI-V). On increasing pressure further to 25 kbar, another phase transition occurs to a previously unobserved form of Sc<sub>2</sub>BDC<sub>3</sub> (with the same topology), which has monoclinic symmetry and crystallizes in the space group *P2<sub>1</sub>/c*.

Both phase transitions change the pore structure of Sc<sub>2</sub>BDC<sub>3</sub>. At 13 kbar, the transition from *Fddd* to *Fdd2* results in an increase from one to three different Sc environments. The tripling of the *b*-axis and lowering in symmetry is driven by the rotation of some of the ScO<sub>6</sub> octahedra, with one rotating clockwise, the other anti-clockwise and the last remaining largely unaltered (Figure 2). On increasing pressure further to 25 kbar, the transition from *Fdd2* to *P2<sub>1</sub>/c* causes a further rotation of the two symmetry independent ScO<sub>6</sub> octahedra. In the final phase, all octahedra are twisted, allowing Sc<sub>2</sub>BDC<sub>3</sub> to adopt a higher density form. Analysis of the subgroup-group relations<sup>[6]</sup> between the three phases shows that the transition from *Fdd2* and *P2<sub>1</sub>/c* symmetry is forbidden and must go via an unobserved intermediate phase.

These structural changes are coupled to a marginal reduction in the percentage pore volume of Sc<sub>2</sub>BDC<sub>3</sub> – reducing from 34.9% to 34.8 % from 10 to 13 kbar respectively, followed by a more significant decrease to 29.2 % in the final phase at 25 kbar. On increasing pressure to 13 kbar, the refined occupancies of the CH<sub>4</sub> molecules decreased, indicating that the amount of CH<sub>4</sub> in the pores started to reduce on undergoing the first phase transition. The driving force for the formation of the high-pressure phases above 10 kbar would therefore appear to be to form denser crystalline phases of Sc<sub>2</sub>BDC<sub>3</sub>, with CH<sub>4</sub> trapped in the pores. Atomic positions for the CH<sub>4</sub> sites were unambiguously determined for all three phases. In both phases, two different sites per channel were maintained, with a similar arrangement to those observed in the original *Fddd* structure. From fully occupied sites in the *Fddd* structure at 10 kbar, half of the sites in the *Fdd2* structure at 13 kbar refine to an occupancy of ca. 0.9, revealing a modest reduction in the number of CH<sub>4</sub> molecules upon increasing pressure (SI-V). Unfortunately, extracting definitive conclusions from the pore content analysis in the *P2<sub>1</sub>/c* phase was not possible, since data quality was seriously compromised at such high-pressures, partly due to CH<sub>4</sub> having frozen around the crystal. For this reason, the above mentioned evidence of a reduction in pore volume is the only indication of reduced pore content in the final *P2<sub>1</sub>/c* phase. On decreasing pressure, and recovering the crystal from the pressure cell, the crystal reverts to the original *Fddd* structure.

Overall, these results highlight the potential of using gases as PTM in high-pressure single-crystal diffraction experiments to explore the maximum gas uptake of porous MOFs at room temperature. Not only is it possible to determine adsorption sites within the pores, but the technique also reveals sites unoccupied

at lower pressures, where low-uptake or large thermal motion may have made determining guest positions within the pores using diffraction techniques extremely challenging, or impossible. These cryogenic loading DAC studies can be of direct relevance to possible applications of MOFs at high pressures, such as UPLC or the storage of mechanical energy.<sup>[17]</sup> Finally, this is a new experimental approach to monitoring gas uptake with associated changes in the framework, which are expected to be widely applicable to other MOFs and help obtain improved atomistic models of the gas molecules inside the pores.

## Acknowledgements

We would like to thank the EPSRC for funding (EP/K033646) and the STFC for awarding beamtime at the Diamond Light Source.

**Keywords:** High-pressure • MOFs • Gas separation • X-ray Crystallography • Structural science

- [1] a) K. Sumida, D. L. Rogow, J. A. Mason, T. M. McDonald, E. D. Bloch, Z. R. Herm, T. H. Bae, J. R. Long, *Chem Rev* **2012**, *112*, 724-781; b) J. R. Li, J. Sculley, H. C. Zhou, *Chem Rev* **2012**, *112*, 869-932.
- [2] A. Greenaway, B. Gonzalez-Santiago, P. M. Donaldson, M. D. Frogley, G. Cinque, J. Sotelo, S. Moggach, E. Shiko, S. Brandani, R. F. Howe, P. A. Wright, *Angewandte Chemie-International Edition* **2014**, *53*, 13483-13487.
- [3] H. C. Hoffmann, M. Debowski, P. Muller, S. Paasch, I. Senkovska, S. Kaskel, E. Brunner, *Materials* **2012**, *5*, 2537-2572.
- [4] E. J. Carrington, I. J. Vitorica-Yrezabal, L. Brammer, *Acta Crystallographica Section B* **2014**, *70*, 404-422.
- [5] a) C. Serre, C. Mellot-Draznieks, S. Surble, N. Audebrand, Y. Filinchuk, G. Ferey, *Science* **2007**, *315*, 1828-1831; b) T. Jacobs, G. O. Lloyd, J.-A. Gertenbach, K. K. Müller-Nedebock, C. Esterhuysen, L. J. Barbour, *Angewandte Chemie International Edition* **2012**, *51*, 4913-4916.
- [6] a) S. Takamizawa, E.-i. Nakata, T. Saito, K. Kojima, *CrystEngComm* **2003**, *5*, 411-413; b) Y.-Q. Tian, Y.-M. Zhao, H.-J. Xu, C.-Y. Chi, *Inorganic Chemistry* **2007**, *46*, 1612-1616; c) J. P. Zhang, X. M. Chen, *J Am Chem Soc* **2009**, *131*, 5516-5521; d) S. Takamizawa, Y. Takasaki, R. Miyake, *Chemical Communications* **2009**, 6625-6627; e) R. Vaidhyanathan, S. S. Iremonger, G. K. H. Shimizu, P. G. Boyd, S. Alavi, T. K. Woo, *Science* **2010**, *330*, 650-653; f) M. Wriedt, J. P. Sculley, A. A. Yakovenko, Y. Ma, G. J. Halder, P. B. Balbuena, H.-C. Zhou, *Angewandte Chemie International Edition* **2012**, *51*, 9804-9808; g) S. Xiang, Y. He, Z. Zhang, H. Wu, W. Zhou, R. Krishna, B. Chen, *Nature Communications* **2012**, *3*, 954; h) S. Couck, E. Gobechiya, C. E. Kirschhock, P. Serra-Crespo, J. Juan-Alcaniz, A. Martinez Joaristi, E. Stavitski, J. Gascon, F. Kapteijn, G. V. Baron, J. F. Denayer, *ChemSusChem* **2012**, *5*, 740-750; i) W. Kosaka, K. Yamagishi, A. Hori, H. Sato, R. Matsuda, S. Kitagawa, M. Takata, H. Miyasaka, *J Am Chem Soc* **2013**, *135*, 18469-18480; j) P. Zhao, G. I. Lampronti, G. O. Lloyd, M. T. Wharmby, S. Facq, A. K. Cheetham, S. A. Redfern, *Chemistry of Materials* **2014**, *26*, 1767-1769; k) W. L. Queen, M. R. Hudson, E. D. Bloch, J. A. Mason, M. I. Gonzalez, J. S. Lee, D. Gygi, J. D. Howe, K. Lee, T. A. Darwish, M. James, V. K. Peterson, S. J. Teat, B. Smit, J. B. Neaton, J. R. Long, C. M. Brown, *Chemical Science* **2014**, *5*, 4569-4581.
- [7] a) M. Eremets, *Hig Pressure Experimental Methods*, Oxford Science Publications, **1996**; b) S. Klotz, J. Chervin, P. Munsch, G. Le Marchand, *Journal of Physics D: Applied Physics* **2009**, *42*, 075413.
- [8] J. Matson, in *Scientific American*, Nature Publishing Group, **2011**.
- [9] N. Pantha, N. P. Adhikari, S. Scandolo, *High Pressure Research* **2015**, 1-8.

- [10] K. W. Chapman, G. J. Halder, P. J. Chupas, *J Am Chem Soc* **2008**, *130*, 10524-10526.
- [11] A. J. Graham, A. M. Banu, T. Duren, A. Greenaway, S. C. McKellar, J. P. S. Mowat, K. Ward, P. A. Wright, S. A. Moggach, *Journal of the American Chemical Society* **2014**, *136*, 8606-8613.
- [12] a) S. A. Moggach, T. D. Bennett, A. K. Cheetham, *Angew Chem Int Ed Engl* **2009**, *48*, 7087-7089; b) D. Fairen-Jimenez, S. A. Moggach, M. T. Wharmby, P. A. Wright, S. Parsons, T. Duren, *J Am Chem Soc* **2011**, *133*, 8900-8902; c) D. Fairen-Jimenez, R. Galvelis, A. Torrisi, A. D. Gellan, M. T. Wharmby, P. A. Wright, C. Mellot-Draznieks, T. Duren, *Dalton Transactions* **2012**, *41*, 10752-10762; d) C. O. Ania, E. García-Pérez, M. Haro, J. J. Gutiérrez-Sevillano, T. Valdés-Solís, J. B. Parra, S. Calero, *J. Phys. Chem. Lett.* **2012**, *3*, 1159-1164.
- [13] S. R. Miller, P. A. Wright, T. Devic, C. Serre, G. Ferey, P. L. Llewellyn, R. Denoyel, L. Guberova, Y. Filinchuk, *Langmuir* **2009**, *25*, 3618-3626.
- [14] H. E. Maynard-Casely, L. F. Lundegaard, I. Loa, M. I. McMahon, E. Gregoryanz, R. J. Nelmes, J. S. Loveday, *The Journal of Chemical Physics* **2014**, *141*, 234313.
- [15] A. J. Graham, D. R. Allan, A. Muszkiewicz, C. A. Morrison, S. A. Moggach, *Angewandte Chemie-International Edition* **2011**, *50*, 11138-11141.
- [16] M. I. Aroyo, J. M. Perez-Mato, D. Orobengoa, E. Tasci, G. de la Flor, A. Kirov, *Bulgarian Chemical Communications* **2011**, *43*, 183-197.
- [17] S.-S. Liu, C.-X. Yang, S.-W. Wang, X.-P. Yan, *Analyst* **2012**, *137*, 816-818.

COMMUNICATION

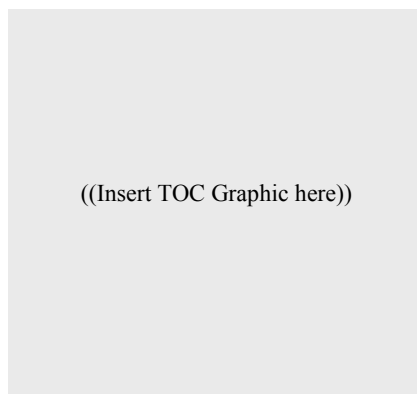
---

Entry for the Table of Contents

COMMUNICATION

---

Text for Table of Contents



*Author(s), Corresponding Author(s)\**

**Page No. – Page No.**

**Title**

WILEY-VCH

---